

RESEARCH PAPER

YC-1 induces apoptosis of human renal carcinoma A498 cells *in vitro* and *in vivo* through activation of the JNK pathway

SY Wu^{1,5}, SL Pan^{1,5}, TH Chen¹, CH Liao¹, DY Huang¹, JH Guh², YL Chang¹, SC Kuo³, FY Lee⁴ and CM Teng¹

¹Department of Pharmacology, College of Medicine, Pharmacological Institute, National Taiwan University, Taipei, Taiwan; ²School of Pharmacy, College of Medicine, National Taiwan University, Taipei, Taiwan; ³Graduate Institute of Pharmaceutical Chemistry, China Medical University, Taichung, Taiwan and ⁴Yung-Shin Pharmaceutical Industry Co. Ltd, Taichung, Taiwan

Background and purpose: The aim of this study was to elucidate the mechanism of YC-1{3-(5'-hydroxy methyl-2'-furyl)-1-benzylindazole}-induced human renal carcinoma cells apoptosis and to evaluate the potency of YC-1 in models of tumour growth in mice.

Experimental approach: YC-1-mediated apoptosis was assessed by analysis of MTT, SRB, DAPI staining and flow cytometry analysis. Knockdown of JNK protein was achieved by transient transfection using siRNA. The mechanisms of action of YC-1 on different signalling pathways involved were studied using western blot. Fas clustering was analysed by confocal microscopy and *in vivo* efficacy was examined in a A498 xenograft model.

Key results: YC-1 displayed cytotoxicity in renal carcinoma cells at 10^{-7} – 10^{-8} M. Increased condensation of chromatin was observed and an increase in the cell population in subG1 phase. Moreover, YC-1 triggered mitochondria-mediated and caspase-dependent pathways. YC-1 significantly induced Fas ligand expression, but did not modify either the protein levels of death receptors or ligands. In addition, Fas clustering in cells responsive to YC-1 was observed, suggesting involvement of a Fas-mediated pathway. Furthermore, YC-1 markedly induced phosphorylation of JNK and a JNK inhibitor, SP600125, and siRNA JNK1/2 significantly reversed YC-1-induced cytotoxicity and protein expression. We suggest that YC-1 induced JNK phosphorylation, the upregulation of FasL and Fas receptor clustering to promote the activation of caspases 8 and 3, resulting in apoptosis. Finally, we demonstrated the antitumour effect of YC-1 *in vivo*.

Conclusions and implications: These data suggest that YC-1 is a good candidate for development as an anticancer drug. *British Journal of Pharmacology* (2008) **155**, 505–513; doi:10.1038/bjp.2008.292; published online 21 July 2008

Keywords: YC-1; renal cancer; apoptosis; JNK

Abbreviations: DAPI, 4',6-diamidino-2-phenylindole; HIF-1 α , hypoxia-inducible factor-1 α ; JNK, Jun N-terminal kinase; MTT assay, 3-(4,5-dimethylthiazol-2-yl)-2,5-diphenyltetrazolium bromide assay; siRNA, small interfering RNA; SP600125, anthra[1-9cd]pyrazol-6(2H)-one; SRB assay, sulphorhodamine B assay

Introduction

Renal cell carcinomas (RCCs) are refractory to most chemotherapies and current therapeutic modalities are of limited efficacy in the treatment of metastatic RCC, which accounts for the one-third of RCC patients at the time of diagnosis (Godley and Taylor, 2001). More recent attempts at treating this disease using growth inhibitory and other immunotherapeutic approaches such as cytokine-based regimens have also proved to be only of marginal benefit (Rohrmann *et al.*, 2005). Therefore, the development of new,

more potent therapies that can more effectively control RCC growth and improve survival is highly desirable.

YC-1, 3-(5'-hydroxy methyl-2'-furyl)-1-benzylindazole, was first discovered in our laboratory where its antiplatelet activity was observed (Ko *et al.*, 1994). More recently, *in vitro* studies showed that YC-1 was able to decrease the accumulation of hypoxia-inducible factor (HIF)-1 α and the expression of downstream HIF-1 target genes, including those for vascular endothelial growth factor and erythropoietin (Chun *et al.*, 2001); YC-1 has also been reported to inhibit angiogenesis and tumour growth in animals (Yeo *et al.*, 2004; Pan *et al.*, 2005). However, the major mechanism of action of YC-1 was found to be its suppression of the PI3K/Akt/mTOR/4E-BP pathway that regulates HIF-1 α expression at the translational step (Sun *et al.*, 2007).

Correspondence: Professor CM Teng, Department of Pharmacology, College of Medicine, National Taiwan University, No. 1, Jen-Ai Road. Section 1, Taipei 100, Taiwan.

E-mail: cmteng@ntu.edu.tw

⁵These authors contributed equally to this work.

Received 26 March 2008; revised 22 May 2008; accepted 4 June 2008; published online 21 July 2008

The two most described pathways for cell death involve the activation of caspase 3 or 7 (Boatright and Salvesen, 2003). Activation of the first pathway, the receptor-mediated pathway, occurs upon engagement of a cell surface receptor with its respective death ligand, resulting in the binding of the adaptor molecule FADD (Fas-associating protein with a death domain) to the receptor (Thorburn, 2004). This results in the recruitment of procaspase 8, the key caspase that distinguishes the receptor-mediated apoptotic pathway. Caspase 8 can then directly activate caspase 3 or 7. The second pathway, the mitochondria-dependent pathway, requires the activation of proapoptotic Bcl-2 family members Bax or Bak, which results in increased permeability of the outer mitochondrial membrane and the subsequent release of proapoptotic proteins, such as cytochrome *c* (Green and Kroemer, 2004). Release of these proteins initiates cell death by caspase-dependent and caspase-independent mechanisms. Caspase 8 may cleave the proapoptotic protein Bid. Truncated Bid activates Bax and/or Bak, resulting in mitochondrial permeability, cytochrome *c* release and downstream caspase activation (Yin, 2000). At present, it is not known which of these cell death pathways are activated by YC-1 in renal cancer cells. This study was undertaken to ascertain whether YC-1 directly induces programmed cell death in renal cancer cells and to define the mechanism(s) whereby this agent could exert its antitumour effects.

Materials and methods

Cell culture

A498 cells (derived from the American Type Culture Collection, Manassas, VA, USA) were cultured in RPMI (Roswell Park Memorial Institute)-1640 medium supplemented with 10% foetal bovine serum and penicillin (100 U mL^{-1})/streptomycin ($100 \mu\text{g mL}^{-1}$). Cultures were maintained in a humidified incubator containing 21% O_2 and 5% CO_2 in air.

Cytotoxicity assay

Cells (1×10^5 cells per well) were incubated in 1 mL of culture medium at 37°C in the presence or absence of YC-1. The assay was terminated and the cell survival was measured by 3-(4,5-dimethylthiazol-2-yl)-2,5-diphenyltetrazolium bromide (MTT) assay as described previously (Pan *et al.*, 2004). Briefly, $100 \mu\text{L}$ MTT solution (0.5 mg mL^{-1} in phosphate-buffered saline; PBS) was added to each well. After 1–2-h incubation at 37°C , $10 \mu\text{L}$ Triton X-100 (10%) was added and mixed well. Absorbance difference at 550 nm was measured using a microplate reader, using RPMI medium as a blank.

Sulphorhodamine B (SRB) assay

Cells were inoculated into 96-well plates (2×10^4 cells per well) in complete media. After overnight culture, cells were cultured in foetal bovine serum-free medium for 24 h followed by pretreatment with various concentrations of YC-1 for 1 h in 0.1% foetal bovine serum culture media. The assay was terminated and the cell growth was measured by

the SRB assay described in a previous study (Wang *et al.*, 2005).

FACScan flow cytometric assay

After the treatment of cells with vehicle (0.1% dimethyl sulphoxide) or compound for the indicated time periods, the cells were harvested by trypsinization, fixed with 70% alcohol at 4°C for 30 min and washed with PBS. After centrifugation, cells were incubated in PBS for 30 min at room temperature. Then the cells were centrifuged and resuspended in a 0.5 mL propidium iodide solution containing Triton X-100 (0.1%, v/v^{-1}), RNase ($100 \mu\text{g mL}^{-1}$) and propidium iodide ($80 \mu\text{g mL}^{-1}$). DNA content was analysed with the FACScan and CellQuest software (Becton Dickinson, Mountain View, CA, USA).

DAPI staining

4'-6-diamidino-2-phenylindole (DAPI), a DNA-binding fluorescent dye, was used to determine whether the mechanism of growth inhibition after YC-1 treatment is through apoptosis. After treatment with YC-1 (0.3, 1 and $3 \mu\text{M}$) for 24 h, the cells were washed three times with PBS, fixed in a 3.7% formaldehyde solution for 10 min, fixed once in 1 mL of methanol and then stained with DAPI for 10 min. Results were determined by visual observation of nuclear morphology through fluorescence microscopy.

Western blot analysis

Total cell lysate was treated with lysis buffer as described previously (Pan *et al.*, 2004). Cell homogenates were diluted with loading buffer and boiled for 5 min to detect phosphorylation, expression and cleavage of proteins. For western blot analysis, proteins (30–60 μg) were separated by electrophoresis in a 10% polyacrylamide gel and transferred to a nitrocellulose membrane. After incubation at room temperature in PBS/5% non-fat milk for 1 h, the membrane was washed thrice with PBS/1% Tween 20. Then the membrane was immunoreacted with primary antibodies overnight at 4°C . After four washings with PBS/1% Tween 20, horseradish peroxidase-conjugated antimouse or antirabbit immunoglobulin G was applied to the membranes for 1 h at room temperature. Finally, the membranes were visualized with an enhanced chemiluminescence kit (Amersham, Buckinghamshire, UK).

Immunofluorescence examination of Fas clustering

Cells were cultured in chamber slides for 24 h and then treated with YC-1 ($3 \mu\text{M}$) for 0.5 and 1 h. After the incubation period, cells were washed twice with PBS and followed by methanol permeabilization for 5 min. The cells were stained with fluorescein isothiocyanate-conjugated cholera toxin for 1 h, and after washout, the primary anti-Fas antibody was used to stain for another 1 h at room temperature. The cells were washed three times with PBS for 15 min. Then, the secondary antibody of tetramethyl rhodamine isothiocyanate-conjugated antimouse immunoglobulin was used. Fas expression was analysed by a confocal laser microscopic system.

Measurement of the change of mitochondrial membrane potential ($\Delta\Psi_m$)

Cells were treated with or without the indicated agent. Thirty minutes before the termination of incubation, rhodamine 123 solution (final concentration of $5\ \mu\text{M}$) was added to the cells and incubated for the last 30 min at 37°C . The cells were finally harvested and the accumulation of rhodamine 123 was determined using FACScan flow cytometric analysis.

siRNA transfection

The target sequence for Jun N-terminal kinase (JNK) 1/2-specific siRNA was 50-AAAAAGAAUGUCCUACCUUCU-30 (Genebank accession number NM002750.2; Gururajan *et al.*, 2005) control siRNA (no silencing) and were synthesized by Invitrogen, Carlsbad, CA, USA. One day before transfection, the cells were plated onto six-well plates with growth medium without antibiotics at a density of 1×10^6 cells per well. Cell transfection was performed by using Opti-MEM media, lipofectamine 2000 and JNK1/2 siRNA according to the manufacturer's recommendations.

Tumour xenograft implantation

BALB/c-nu mice were maintained and all animal procedures were in accordance with the Institutional Animal Care and Use Committee procedures and guidelines. Male BALB/c-nu mice (20 g, 4 weeks of age) were obtained from National Laboratory Animal Center, Taiwan, and acclimatized to laboratory conditions for 1 week before tumour implantation. The BALB/c-nu mice were injected s.c. with human renal cancer A498 (10^7 cell/mouse) into the flank of each animal. At 32 days after the inoculation of cancer cells, when the tumours had grown to the size of around 80 to $100\ \text{mm}^3$, the animals were divided into four groups. Both vehicle and YC-1 were suspended in 0.5% carboxymethyl cellulose and then vehicle or YC-1 (10 , 30 and $100\ \text{mg kg}^{-1}\ \text{day}^{-1}$) was given orally every day from the 32nd day, and tumour size was measured every 3–4 days. The animals were killed by intraperitoneal injection of pentobarbital on the 56th day. The tumours were carefully removed and weighed. Tumour volume was determined by measuring the largest diameters (l) and the smallest diameters (s), and the volumes were calculated ($V = 0.5ls^2$).

In situ analysis of tumour tissue sections by immunohistochemistry and immunofluorescence

Renal tumours harvested at autopsy were processed for immunohistochemistry using an antibody, which recognizes the activated form of phospho-JNK. Briefly, $5\ \mu\text{m}$ paraffin sections were deparaffinized and endogenous peroxidase was destroyed with 3% H_2O_2 in 100% methanol. Non-specific antigenic sites were blocked with 3% bovine serum albumin in PBS for 30 min at room temperature. Tissues were incubated with a monoclonal antibody, which recognized phospho-JNK, overnight at 4°C . Negative controls were carried out using non-specific immunoglobulin G. A standard LSAB technique (DAKO, Glostrup, Denmark) was used to detect the reaction products.

Statistical analysis

Data are presented as mean \pm s.e. mean and analysed statistically by using one-way ANOVA. When ANOVA showed significant differences between groups, Tukey's *post hoc* test was used to determine the specific pairs of groups between which statistically significant differences occurred. $P < 0.05$ was the accepted level for statistical significance.

Materials

YC-1 was obtained from Yung-Shin Pharmaceutical Industry Co. Ltd (Taichung, Taiwan). RPMI-1640 medium, foetal bovine serum, penicillin and streptomycin were obtained from Gibco BRL Life Technologies (Grand Island, NY, USA). Propidium iodide, DAPI dihydrochloride, MTT, SP600125, dimethyl sulphoxide, leupeptin, dithiothreitol, reagent, phenylmethylsulphonyl fluoride, SRB and fluorescein isothiocyanate-conjugated antimouse immunoglobulin G were obtained from Sigma (St Louis, MO, USA). The caspase inhibitor z-VAD-fmk was purchased from BACHEM AG (King of Prussia, PA, USA). All antibodies and antimouse and antirabbit immunoglobulin Gs were obtained from Santa Cruz Biotechnology Inc. (Santa Cruz, CA, USA).

Results

YC-1 is cytotoxic to human renal cancer cell lines

We first determined the effect of YC-1 on the growth of human renal cancer cell lines using the MTT assay. YC-1 was significantly cytotoxic in all the four cell lines (A498, ACHN, UO-31 and 8701) tested, with the most potent effects being observed in A498 cells ($\text{IC}_{50} = 1.9 \times 10^{-7}\ \text{M}$) (Figure 1a). In addition, we also found that YC-1 inhibits cell growth of A498 cells in a concentration-dependent fashion, with IC_{50} of $8.3 \times 10^{-8}\ \text{M}$ (Figure 1b). Cell cycle distributions were analysed by flow cytometry to determine whether YC-1-induced cytotoxicity was associated with a disturbance of cell cycle regulation. Accumulation of vehicle-treated A498 cells occurred at the G0/G1 phase (Figure 1c). Treatment of cells with YC-1 resulted in an increase in the percentage of cells in the sub-G1 phase. This increase occurred in a time-dependent manner indicative of apoptosis and consistent with the induction of cell death.

The mode of induction of YC-1-induced cell death was also examined by DAPI staining using immunofluorescence microscopy (Figure 1d). YC-1 significantly increased the condensation of chromatin, suggesting apoptosis.

YC-1 induces apoptosis associated with PARP, caspases 8 and 3 cleavage

We further characterized apoptosis triggered by YC-1 by examining cleavage of poly(ADP-ribose) polymerase (PARP) as well as caspases 8 and 3 in A498 cells. A498 cells were exposed to YC-1 at for the times indicated, and cell lysates were then examined by western blotting. Both time-course (Figure 2a) and concentration-response (Figure 2b) experiments showed that YC-1 induced significant (PARP), caspases 8 and 3 cleavages. Finally, to confirm the role played by caspases in YC-1-induced apoptosis, A498 cells

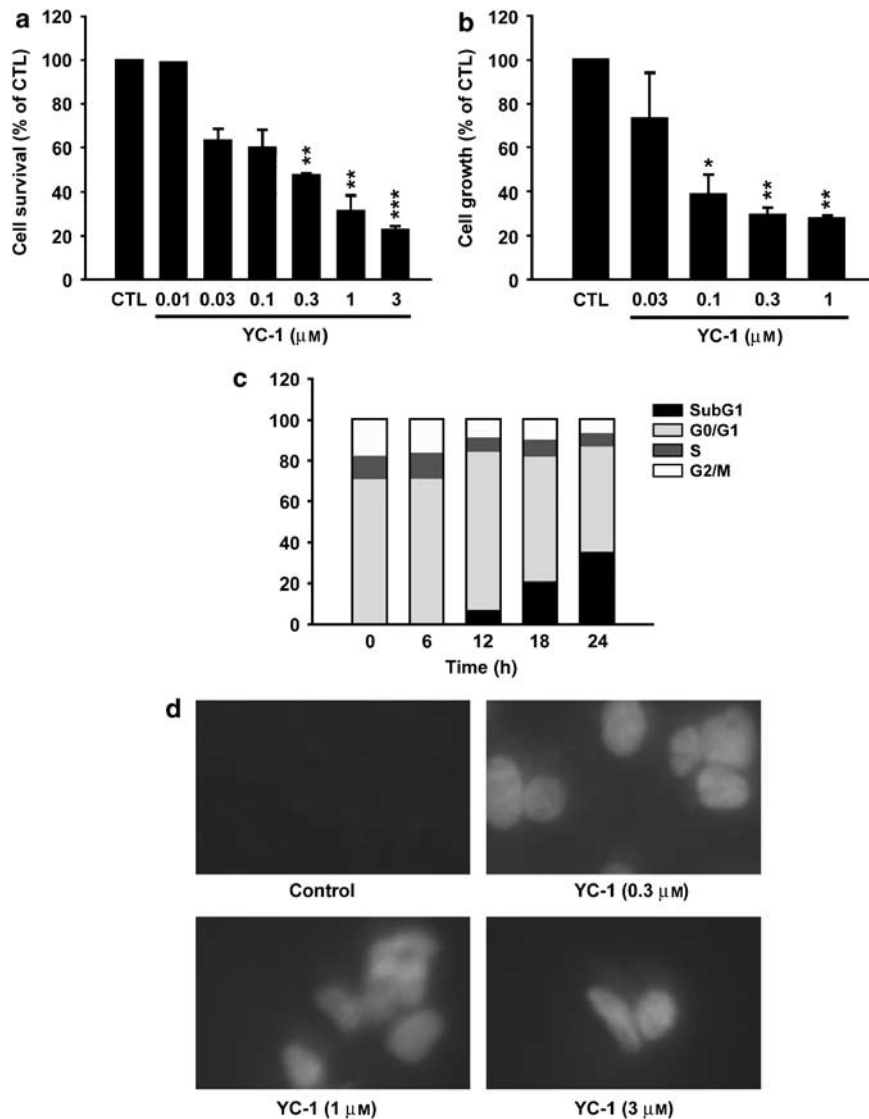


Figure 1 Effect of YC-1-induced cytotoxicity in human renal cancer A498 cells. Cells were incubated in the absence (control; CTL) or presence of YC-1, in serum-containing medium for 24 h (MTT assay) or 48 h (SRB assay). The cytotoxic effect (a) was determined using the MTT assay and the antiproliferative effect (b) was determined using the SRB assay. (c) The cell cycle progression and cell apoptosis were determined using FACS analysis as described in Materials and methods section. (d) Fluorescence microscopic examination of untreated or YC-1 treated at the indicated concentrations for 24 h followed by DAPI staining. YC-1 significantly induced chromatin condensation and nuclei fragmentation. Magnification $\times 40$. * $P < 0.05$, ** $P < 0.01$ and *** $P < 0.001$ compared with the control group. DAPI, 4',6-diamidino-2-phenylindole; MTT, 3-(4,5-dimethylthiazol-2-yl)-2,5-diphenyltetrazolium bromide; SRB, sulphorhodamine B.

were pretreated with the pan-caspase inhibitor, z-VAD-fmk, for 1 h and then treated with YC-1 (0.3 μM) for 24 h. YC-1-induced cell death was significantly inhibited by z-VAD-fmk (Figure 2c). On the basis of these results, we conclude that YC-1-induced apoptosis is, at least in part, mediated by caspases.

Intrinsic apoptotic pathway proteins are modulated during YC-1-induced apoptosis

The Bcl-2 protein family is involved in regulating apoptotic cell death. Bcl-2 protein and other antiapoptotic members of the Bcl-2 family are important for maintaining mitochondrial membrane integrity (Willis *et al.*, 2003). Because YC-1 activates caspase 3, which is also a mitochondria-mediated

caspase, we sought to determine whether YC-1 would affect the protein levels of these Bcl-2 family members. Significant changes were detected in expression of both the proapoptotic family member Bax, and the antiapoptotic members Bcl-2 and Bcl-xl after YC-1 treatment (Figure 3a). In addition, because the mitochondria are key organelles in the control of apoptosis, we investigated whether YC-1 was capable of inducing depolarization of the mitochondrial transmembrane potential ($\Delta\Psi_m$) using rhodamine 123, a mitochondrial-specific and voltage-dependent dye. The results indicated that the treatment of A498 cells with YC-1 induced dissipation of $\Delta\Psi_m$ in a time-dependent manner (Figure 3b). Moreover, it is well known that the dissipation of $\Delta\Psi_m$ causes release of cytochrome *c*, apoptosis-inducing factor, and second mitochondrial activator of caspases/direct

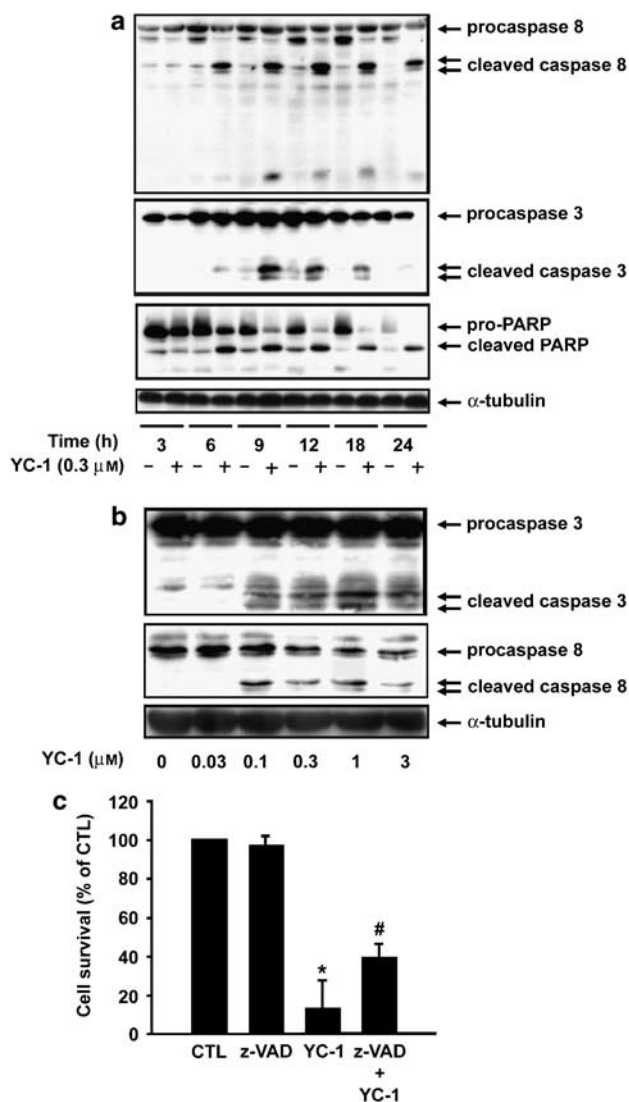


Figure 2 YC-1 induces caspase activation and cleaves the caspase substrate, PARP. A498 cells were incubated in the absence or presence of YC-1 for the times indicated (a) or at varying concentration (b). The cells were harvested and prepared for detection of pro-caspases 3, 8 and PARP expression using western blotting. (c) A498 cells were preincubated in the absence or presence of z-VAD-fmk (30 μ M) for 1 h, and then YC-1 (0.3 μ M) was added to the cells for 24 h. The cytotoxic effect was determined using MTT assay. Data represent the mean \pm s.e.mean from four independent experiments. * P <0.05 as compared with the control group, # P <0.05 as compared with the YC-1-treated group. MTT, 3-(4,5-dimethylthiazol-2-yl)-2,5-diphenyltetrazolium bromide.

IAP (inhibitor of apoptosis) binding protein with low pI (Smac/DIABLO) into the cytosol, with consequent activation of the execution phase of apoptosis (Saelens *et al.*, 2004). In this study, we demonstrated that mitochondrial cytochrome *c*, but not apoptosis-inducing factor or Smac/DIABLO, was released into the cytosol during YC-1 (0.3 μ M)-induced apoptosis (Figure 3c), demonstrating a putative involvement of the mitochondrial pathway. These results suggest that YC-1-induced apoptosis involves the mitochondria-dependent pathway in A498 cells.

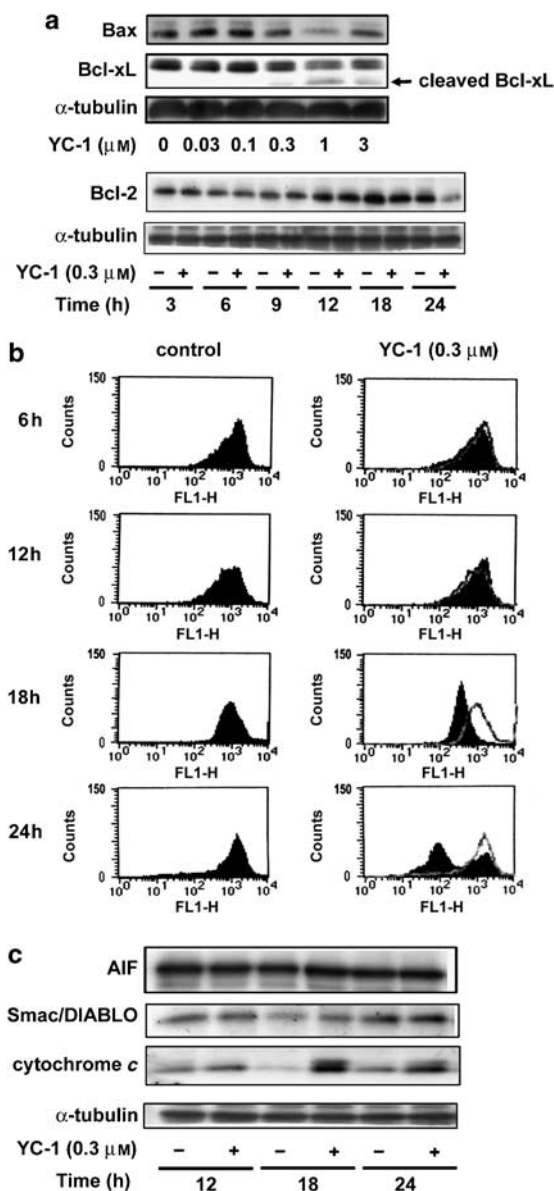


Figure 3 The intrinsic apoptotic pathway proteins are modulated during YC-1-induced apoptosis. A498 cells were incubated in the absence or presence of YC-1 for 24 h, and cells were harvested and prepared for the detection of Bcl-2 family expression (a) using western blot analysis as described in Materials and methods section. (b) The mitochondria transmembrane potential was determined using FACS analysis. (c) Apoptosis-inducing factor, Smac/DIABLO and cytochrome *c* released from mitochondria was determined by western blot analysis.

Effects of YC-1 on death receptors and expression of their ligands Death receptors, on binding to their ligands, trigger apoptosis by stimulating the caspase 8-mediated caspase cascades. In this study, expression of several death receptors (Fas, DR4 and DR5) and their ligands (FasL and Apo-2L/TRAIL) were detected in A498 cells (Figures 4a and b). However, treatment with YC-1 did not modify the expression of death receptors and TRAIL, although it increased the expression of FasL in a concentration- and time-dependent manner (Figures 4a and c). However, it has also been

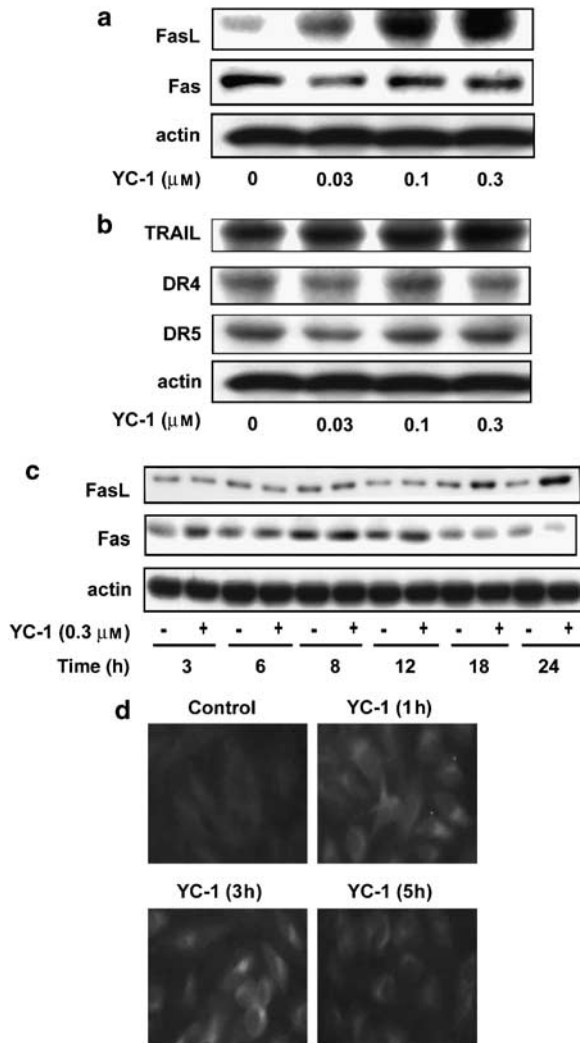


Figure 4 Effect of YC-1 on death receptors and their ligand expression and the aggregation state of Fas. (a and b) A498 cells were incubated in the absence or presence of YC-1 for 24 h or (c) for the times indicated. The cells were harvested and prepared for the detection of death receptors and their ligands. (d) A498 cells were either untreated or treated with YC-1 (0.3 μM) for the times indicated. Cells were prepared for the detection of Fas clustering phenomena. The procedures used are described in Materials and methods. Magnification $\times 400$.

suggested that the Fas-mediated effect is not only regulated by its associated ligand, but also by ligand-independent activation of the death receptor (Gajate *et al.*, 2000). Increasing evidence indicates that the clustering of Fas in lipid rafts has been shown in apoptosis triggering, involving caspase 8 and Bid downstream signalling (Gajate *et al.*, 2004). In this study, confocal immunofluorescence microscopic examination showed that membrane-bound Fas was detected in diffused and buoyant locations in control cells. YC-1 caused rapid redistribution and clustering of Fas at the indicated times (Figure 4d). Taken together, these findings suggest that YC-1 activates an extrinsic pathway of FasL and the Fas clustering pathway to induce apoptotic cell death in A498 cells.

YC-1-induced apoptosis is mediated via JNK pathway

In previous studies, investigators have reported that JNK induces cell apoptosis (Kanda and Miura, 2004; Liu and Lin, 2005). Therefore, we determined whether JNK was activated by YC-1 in A498 cells. Our results show that YC-1 induced significant JNK activation in A498 cells early after exposure to YC-1 (0.3 μM) (Figure 5a). Notably, significant rescue from cell death was observed when A498 cells were treated with JNK inhibitor SP600125 before YC-1 treatment. SP600125 reduced A498 cell death by $\sim 50\%$ (Figure 5b). SP600125 alone exhibited no cytotoxic effects on A498 cells at the doses used. Moreover, SP600125 also blocked YC-1-induced JNK activity (Figure 5c) and caspase 8 (Figure 5d). Activation of JNK in response to YC-1 was not associated with changes in total internal control of α -tubulin. To determine whether the activation of JNK would be required for YC-1-induced cell apoptosis, an alternative approach using siRNA directed against a common sequence of JNK1/2, was utilized to inhibit JNK expression. Transient transfection with siRNA led to the efficient downregulation of JNK1/2 (Figure 5e), and significantly prevented cell apoptosis. siRNA transfection also reduced phosphorylation of JNK, total JNK and caspase 8 cleavage induced by YC-1 when evaluated using the MTT assay and western blot analysis, respectively. These results suggest that JNK functions as a proapoptotic effector kinase in YC-1-induced apoptosis in A498 cells, and that YC-1-mediated apoptosis is, at least in part, mediated by the JNK pathway.

YC-1 inhibits tumour growth in the mouse xenograft model of A498

On the basis of the YC-1-induced apoptotic effect exhibited *in vitro*, we decided to determine whether YC-1 possessed antitumour activities *in vivo*. We established xenografts of A498 cells in nude mice; as tumours reached 100 mm^3 in size, the mice were divided into four groups and orally treated with either vehicle or YC-1. YC-1 induced a dose-dependent inhibition of tumour growth (Figure 6a). Furthermore, we observed little difference in body weight between controls and YC-1-treated animals, indicating that YC-1 had minimal toxicity *in vivo* (Figure 6b). Finally, *ex vivo* analysis of tumours excised from mice showed significantly increased apoptosis in the YC-1-treated group compared with that in the control group, as shown by H&E staining and immunohistochemistry for phospho-JNK (Figure 6c). YC-1 induced a significant reduction in phospho-JNK staining cells, confirming the *in vivo* apoptotic effect of YC-1. Taken together, these results suggest that YC-1 inhibits tumour growth by inducing A498 cell apoptosis *in vivo*.

Discussion and conclusions

Renal cancer is the most lethal of the common urological malignancies. Current therapy is inadequate as shown by the poor 5-year survival rates of patients with metastatic disease. Since a significant disparity exists in the survival of patients with localized versus metastatic disease, efforts are underway to target novel therapeutic approaches against this aspect of the disease. YC-1 was initially identified as a

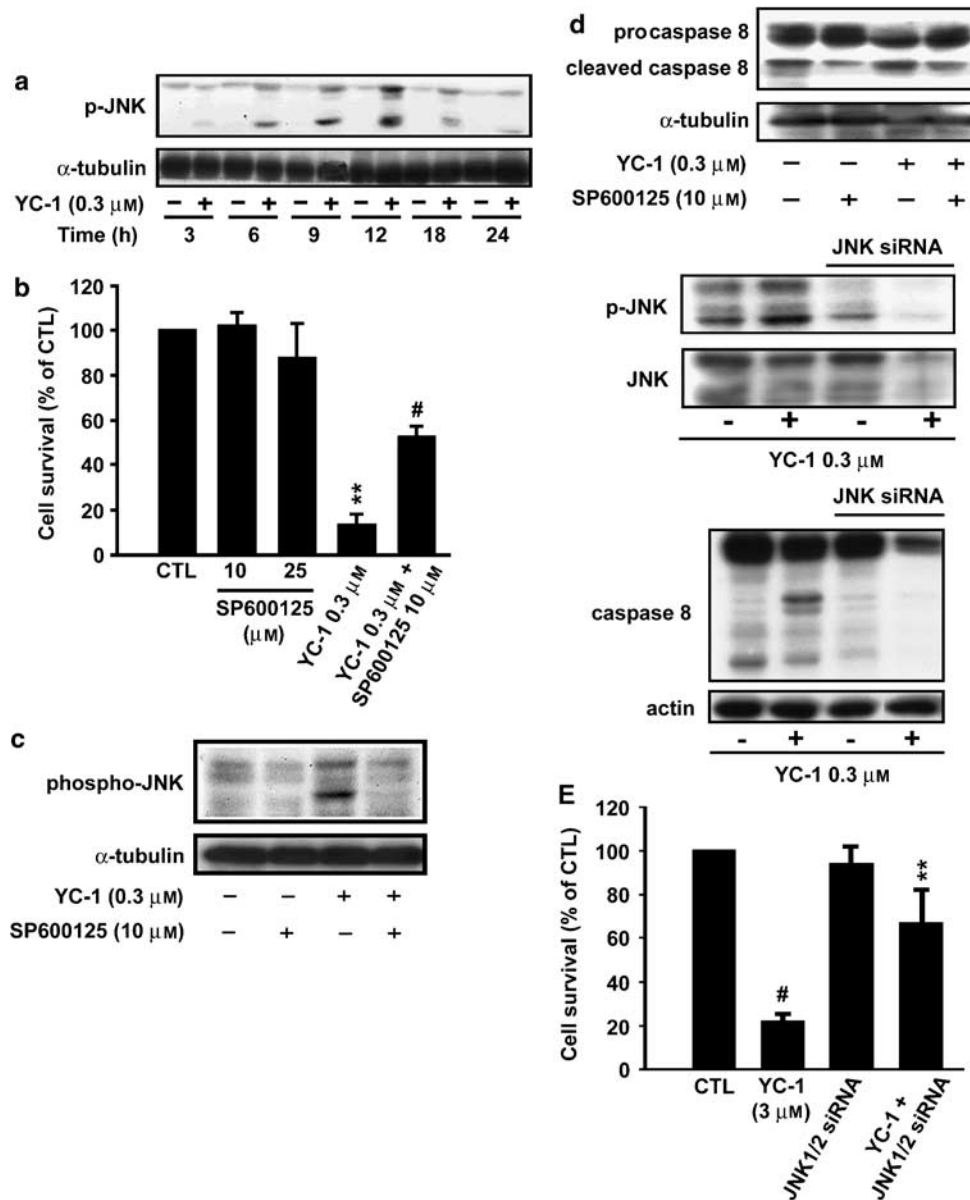


Figure 5 YC-1-induced apoptosis is mediated through JNK pathway. A498 cells were incubated in the absence or presence of YC-1 (0.3 μ M) for the times indicated, and cells harvested and prepared for the detection of phospho-JNK and internal control α -tubulin expression using western blot analysis. (b) Cells were preincubated in the absence or presence of SP600125 for 1 h, and then YC-1 was added to the cells for 24 h. The cytotoxic effect was determined using MTT assay method as described in Materials and methods section. ** $P < 0.01$ as compared with the control group, # $P < 0.05$ as compared with the YC-1-treated group. Cells were preincubated in the absence or presence of SP600125 for 1 h, and then YC-1 was added to the cells for 24 h. The activation of phosphorylation of JNK (c) and caspase 8 (d) were detected by western blot analysis. (e) A498 cells were transfected with JNK1/2 siRNA and placed in 96-well plates 3 days after transfection. Cell viability, phospho-JNK, total JNK and caspase 8 were assayed as described in Materials and methods section. Data are the mean \pm s.e.mean of three independent experiments. # $P < 0.001$ and ** $P < 0.01$ versus YC-1-treated groups. JNK, Jun N-terminal kinase; MTT, 3-(4,5-dimethylthiazol-2-yl)-2,5-diphenyltetrazolium bromide.

unique NO-independent, NO-enhancing activator of sGC; it has been used as a research tool for characterization of NO/sGC/cGMP signalling and function in various tissues. (Ko *et al.*, 1994; Wu *et al.*, 1995; Hwang *et al.*, 2003). Recently, alternative mechanisms of action have been proposed to account for the antitumour effect of YC-1 and many studies have been initiated to explore the antitumour efficacy of YC-1 *in vivo* (Huang *et al.*, 2005; Wang *et al.*, 2005). In addition, the cytotoxic activity of YC-1 has been

evaluated on 39 types of cancer cell lines in a study conducted by the Japanese National Cancer Institute; YC-1 showed more selective cytotoxicity on renal cancer cells, with IC₅₀ of 8.3×10^{-8} M. Hence, in our study, we wished to clarify the mechanisms of action of YC-1-mediated anti-tumour activity in A498 human renal cancer cells both *in vitro* and *in vivo*.

YC-1 induced significant, concentration-dependent growth inhibition and apoptosis, as well as accumulation

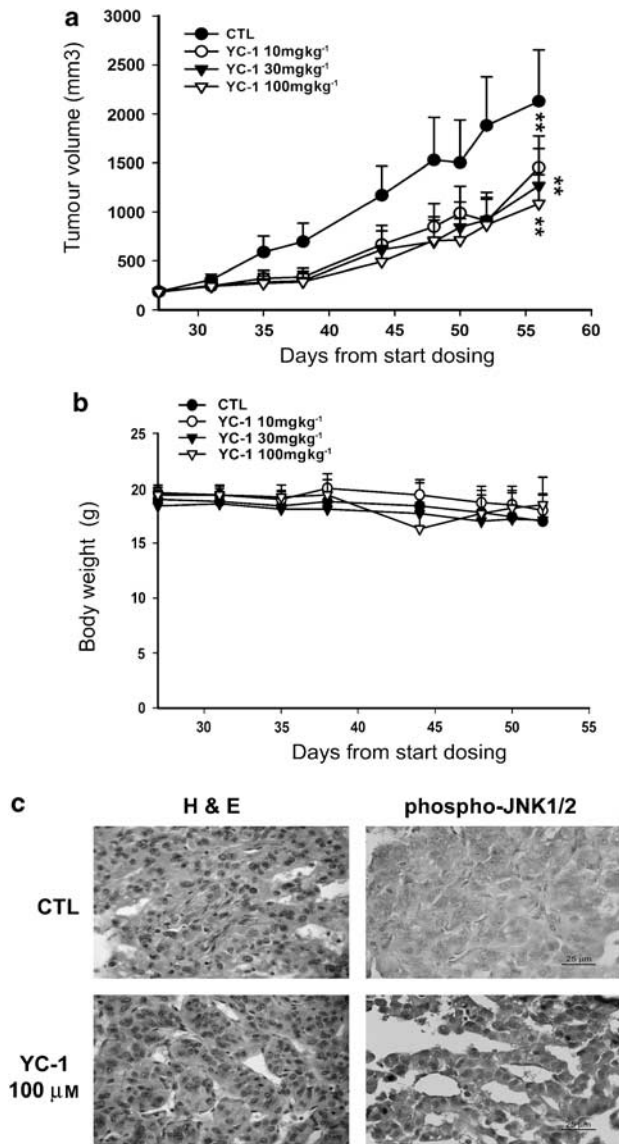


Figure 6 Effect of YC-1 on human renal cancer xenografts. Mice were injected s.c. with A498 tumour cells. After the tumours reached 80–100 mm³ in size, YC-1 (10–100 mg kg⁻¹) or vehicle (0.5% carboxymethyl cellulose) was orally administered daily for 4 weeks. (a) The s.c. tumour volume of A498 cells exceeded 2000 mm³ in size in the control group. Points represent a mean of data obtained from seven mice. (b) Quantitation of body weight from vehicle- and YC-1-treated mice. Each value represents the mean of at least seven animals. ***P* < 0.01 compared with the control group. (c) Protein expression of phospho-JNK1/2 was detected using immunohistochemical analyses as described in Materials and methods. JNK, Jun N-terminal kinase.

in sub-G1 phase and chromatin condensation in A498 human renal cancer cells as evaluated by the DAPI assay.

We found that YC-1 modulates both intrinsic and extrinsic apoptotic pathway proteins in A498 cells, as shown by changes in the expression of Bcl-2 family members, as well as expression of the Fas ligand and Fas clustering effect. In addition, YC-1 triggers caspase activation and also induces the release of cytochrome *c* and mediators of caspases-dependent apoptotic pathway into the cytosol. Moreover, z-VAD-fmk significantly inhibits YC-1-induced cell death.

These results suggest the involvement of both extrinsic and intrinsic apoptotic cascades in YC-1-treated A498 cancer cells.

The von Hippel-Lindau (VHL) tumour-suppressor gene is mutated or silenced in most clear RCCs (Kim and Kaelin, 2004). Loss of the VHL protein (pVHL) results in the stabilization of the heterodimeric transcription factor, HIF and enhanced transactivation of HIF target genes. Down-regulation of HIF is both necessary and sufficient for pVHL to suppress the growth of human renal carcinoma cells in preclinical models. In a previous study, we showed that YC-1 inhibited HIF-1 α activity and protein expression, resulting in antiangiogenic and antitumour growth effects (Yeo *et al.*, 2004). However, the major mechanism of YC-1 action was the suppression of the PI3K/Akt/mTOR/4E-BP pathway, which serves to regulate HIF-1 α expression at the translational step (Sun *et al.*, 2007). Other studies have demonstrated that JNK activity (Seko *et al.*, 1997; Jin *et al.*, 2000) was involved in hypoxia-induced apoptosis (Garay *et al.*, 2000; Kunz *et al.*, 2001) through activator protein-1 and c-jun (Minet *et al.*, 2001). However, JNK activation correlated positively with HIF-1-dependent transcription. In this study, we demonstrated that the JNK pathway was involved in the differential effect of YC-1 in human renal cancer A498 cells. YC-1 had a major effect on the activation of JNK, but not on ERK and p38 MAPKs (data not shown). Significant attenuation of cell apoptosis, phosphorylation of JNK, total JNK, and caspase 8 activity by SP600125, a JNK inhibitor, or JNK siRNA, suggests that JNK is involved in modulating RCC cytotoxicity by YC-1. These observations support the possibility that JNK activation, when HIF-1 is overexpressed in RCC cells, increases the sensitivity to YC-1 in causing cell death.

Induction of transcription of the Fas ligand (FasL) is a key component of the apoptotic pathway mediated through the SAPK/JNK signalling cascade (Faris *et al.*, 1998a and b) and leading to the activation of activator protein-1. Binding of FasL and TRAIL to their respective receptors leads to the activation of downstream apoptotic signals (Scaffidi *et al.*, 1998). The expression of several death receptors (Fas, DR4 and DR5) and their ligands (FasL and TRAIL) were detected in this study, suggesting an upstream effector mechanism in the triggering of the activation of caspase 8. Data showed that the protein level of FasL was altered by YC-1. The crucial role of Fas clustering in apoptosis has also been implicated in the response to multiple apoptotic stimuli in several tumour types (Gajate *et al.*, 2000). Therefore, we also analysed whether YC-1 could induce Fas clustering. Our data showed that the aggregation of Fas occurred within 30 min after exposure of cells to YC-1. These results indicate that YC-1-induced apoptosis through FasL-dependent (increased FasL expression) and FasL-independent (Fas clustering) pathways. Our data also showed that FasL expression/Fas clustering, caspase 8 activation and the activation of caspase 3 were linked in the signalling cascade. Taken together, YC-1 acts in a different and unique way by activating the JNK/FasL/caspase 8 pathway in A498 cells.

In conclusion, we have evaluated YC-1 for its anticancer effect on human renal cancer A498 cells. YC-1 showed high cytotoxic potency in A498 cells. YC-1 induced apoptosis

by inducing Bax to the mitochondria and depolarizing the mitochondrial membrane. Our analysis of upstream signaling revealed that YC-1 activates the JNK pathway in its induction of apoptosis; treatment with a JNK inhibitor and siRNA JNK were able to inhibit the cytotoxicity of YC-1. Furthermore, YC-1 significantly inhibited the growth of s.c. xenograft tumours. Our results suggest that YC-1 may be a promising candidate for use as an antirenal cancer drug.

Acknowledgements

This study was supported by a grant from the National Science Council of Taiwan (NSC 96-2628-B-002-109-MY3) and (NSC 96-2628-B-002-108-MY2).

Conflict of interest

The authors state no conflict of interest.

References

- Boatright KM, Salvesen GS (2003). Mechanisms of caspase activation. *Curr Opin Cell Biol* 15: 725–731.
- Chun YS, Yeo EJ, Choi E, Teng CM, Bae JM, Kim MS *et al.* (2001). Inhibitory effect of YC-1 on the hypoxic induction of erythropoietin and vascular endothelial growth factor in Hep3B cells. *Biochem Pharmacol* 61: 947–954.
- Faris M, Kokot N, Latinis K, Kasibhatla S, Green DR, Koretzky GA *et al.* (1998b). The c-Jun N-terminal kinase cascade plays a role in stress-induced apoptosis in Jurkat cells by up-regulating Fas ligand expression. *J Immunol* 160: 134–144.
- Faris M, Latinis KM, Kempiak SJ, Koretzky GA, Nel A (1998a). Stress-induced Fas ligand expression in T cells is mediated through a MEK kinase 1-regulated response element in the Fas ligand promoter. *Mol Cell Biol* 18: 5414–5424.
- Gajate C, Del Canto-Janez E, Acuna AU, Amat-Guerri F, Geijo E, Santos-Beneit AM *et al.* (2004). Intracellular triggering of Fas aggregation and recruitment of apoptotic molecules into Fas-enriched rafts in selective tumor cell apoptosis. *J Exp Med* 200: 353–365.
- Gajate C, Fonteriz RI, Cabaner C, Alvarez-Noves G, Alvarez-Rodriguez Y, Modolell M *et al.* (2000). Intracellular triggering of Fas, independently of FasL, as a new mechanism of antitumor ether lipid-induced apoptosis. *Int J Cancer* 85: 674–682.
- Garay M, Gaarde W, Monia BP, Nero P, Cioffi CL (2000). Inhibition of hypoxia/reoxygenation-induced apoptosis by an antisense oligonucleotide targeted to JNK1 in human kidney cells. *Biochem Pharmacol* 59: 1033–1043.
- Godley PA, Taylor M (2001). Renal cell carcinoma. *Curr Opin Oncol* 7: 199–203.
- Green DR, Kroemer G (2004). The pathophysiology of mitochondrial cell death. *Science* 305: 626–629.
- Gururajan M, Chui R, Karuppanan AK, Ke J, Jennings CD, Bondada S (2005). c-Jun N-terminal kinase (JNK) is required for survival and proliferation of B-lymphoma cells. *Blood* 106: 1382–1391.
- Huang YT, Pan SL, Guh JH, Chang YL, Lee FY, Kuo SC *et al.* (2005). YC-1 suppresses constitutive nuclear factor-kappaB activation and induces apoptosis in human prostate cancer cells. *Mol Cancer Ther* 4: 1628–1635.
- Hwang TL, Wu CC, Guh JH, Teng CM (2003). Potentiation of tumor necrosis factor-alpha expression by YC-1 in alveolar macrophages through a cyclic GMP-independent pathway. *Biochem Pharmacol* 66: 149–156.
- Jin N, Hatton N, Swartz DR, Xia X, Harrington MA, Larsen SH *et al.* (2000). Hypoxia activates jun-N-terminal kinase, extracellular signal-regulated protein kinase, and p38 kinase in pulmonary arteries. *Am J Respir Cell Mol Biol* 23: 593–601.
- Kanda H, Miura M (2004). Regulatory roles of JNK in programmed cell death. *J Biochem (Tokyo)* 136: 1–6.
- Kim WY, Kaelin WG (2004). Role of VHL gene mutation in human cancer. *J Clin Oncol* 22: 4991–5004.
- Ko FN, Wu CC, Kuo SC, Lee FY, Teng CM (1994). YC-1, a novel activator of platelet guanylate cyclase. *Blood* 84: 4226–4233.
- Kunz M, Ibrahim S, Koczan D, Thiesen HJ, Köhler HJ, Acker T *et al.* (2001). Activation of c-Jun NH2-terminal kinase/stress-activated protein kinase (JNK/SAPK) is critical for hypoxia-induced apoptosis of human malignant melanoma. *Cell Growth Differ* 12: 137–145.
- Liu J, Lin A (2005). Role of JNK activation in apoptosis: a double-edged sword. *Cell Res* 15: 36–42.
- Minet E, Michel G, Mottet D, Piret JP, Barbieux A, Raes M *et al.* (2001). c-JUN gene induction and AP-1 activity is regulated by a JNK-dependent pathway in hypoxic HepG2 cells. *Exp Cell Res* 265: 114–124.
- Pan SL, Guh JH, Chang YL, Kuo SC, Lee FY, Teng CM (2004). YC-1 prevents sodium nitroprusside-mediated apoptosis in vascular smooth muscle cells. *Cardiovasc Res* 61: 152–158.
- Pan SL, Guh JH, Peng CY, Wang SW, Chang YL, Cheng FC *et al.* (2005). YC-1 [3-(5'-hydroxymethyl-2'-furyl)-1-benzyl indazole] inhibits endothelial cell functions induced by angiogenic factors *in vitro* and angiogenesis *in vivo* models. *J Pharmacol Exp Ther* 314: 35–42.
- Rohrmann K, Staehler M, Haseke N, Bachmann A, Stief CG, Siebels M (2005). Immunotherapy in metastatic renal cell carcinoma. *World J Urol* 23: 196–201.
- Saelens X, Festjens N, Vande Walle L, van Gurp M, van Loo G, Vandenabeele P (2004). Toxic proteins released from mitochondria in cell death. *Oncogene* 23: 2861–2874.
- Scaffidi C, Fulda S, Srinivasan A, Friesen C, Li F, Tomaselli KJ *et al.* (1998). Two CD95 (APO-1/Fas) signaling pathways. *EMBO J* 17: 1675–1687.
- Seko Y, Takahashi N, Tobe K, Kadowaki T, Yazaki Y (1997). Hypoxia and hypoxia/reoxygenation activate p65PAK, p38 mitogen-activated protein kinase (MAPK), and stress-activated protein kinase (SAPK) in cultured rat cardiac myocytes. *Biochem Biophys Res Commun* 239: 840–844.
- Sun HL, Liu YN, Huang YT, Pan SL, Huang DY, Guh JH *et al.* (2007). YC-1 inhibits HIF-1 expression in prostate cancer cells: contribution of Akt/NF-kappaB signaling to HIF-1alpha accumulation during hypoxia. *Oncogene* 26: 3941–3951.
- Thorburn A (2004). Death receptor-induced cell killing. *Cell Signal* 16: 139–144.
- Wang SW, Pan SL, Guh JH, Chen HL, Huang DM, Chang YL *et al.* (2005). YC-1 [3-(5'-Hydroxymethyl-2'-furyl)-1-benzyl Indazole] exhibits a novel antiproliferative effect and arrests the cell cycle in G0-G1 in human hepatocellular carcinoma cells. *J Pharmacol Exp Ther* 312: 917–925.
- Willis S, Day CL, Hinds MG, Huang DC (2003). The Bcl-2-regulated apoptotic pathway. *J Cell Sci* 116: 4053–4056.
- Wu CC, Ko FN, Kuo SC, Lee FY, Teng CM (1995). YC-1 inhibited human platelet aggregation through NO-independent activation of soluble guanylate cyclase. *Br J Pharmacol* 116: 1973–1978.
- Yeo EJ, Chun YS, Park JW (2004). New anticancer strategies targeting HIF-1. *Biochem Pharmacol* 68: 1061–1069.
- Yin XM (2000). Signal transduction mediated by Bid, a pro-death Bcl-2 family proteins, connects the death receptor and mitochondria apoptosis pathways. *Cell Res* 10: 161–167.